Large-Scale Production of Single-walled Carbon Nanotubes using Ultrafast Pulses from a Free Electron Laser

P.C. Eklund*, B.K. Pradhan, U. J. Kim

Dept. of Physics, The Pennsylvania State University, University Park, PA16802

J.E. Fischer

Dept of Materials Science and Engineering and LRSM, University of Pennsylvania, Philadelphia, PA 19104

A.D. Friedman and B.C. Holloway,

Dept. of Applied Science, College of William and Mary, Williamsburg, VA 23187

K. Jordan

Thomas Jefferson National Accelerator Facility, Newport News, , VA 23606

M. W. Smith,

NASA Langley Research Center, Hampton, VA 23681

We report very high production rates of SWNTs from carbon vapor produced by *ultrafast* (~0.5 ps) pulsed infrared radiation from the Free Electron Laser (FEL) at the Thomas Jefferson National Accelerator (Jlab). To harness the high average power (~ 1 kW average power) of this FEL beam, a new vaporization geometry was developed in which the laser radiation impinges on the sidewall of a translating and spinning, carbon rod. Using only 30% of the available FEL average power at a wavelength of ~3 microns, we have been able to generate carbon soots rich in bundles of SWNTs at the rate of ~ 1.5 gm/h. Samples were characterized by scanning electron microscope (SEM), transmission electron microscopy (TEM), Temperature programmed oxidation (TPO), and Raman spectroscopy.

* Corresponding Author: pce3@psu.edu

Since the first reports of the single-walled carbon nanotube (SWNT) in 1991 by researchers at NEC and IBM Almaden [1,2], different synthesis routes, such as the Arc Discharge (AD) [1,2,3], Pulsed Laser Vaporization (PLV) [4], and Chemical Vapor Deposition (CVD) [5, 6] methods, have been developed to improve both the production rate and fractional conversion of the carbon feedstock to SWNTs. In the ensuing ten years since their discovery, catapulted forward by the pioneering PLV work at Rice University [4], SWNTs have been the subject of intense worldwide fundamental research and development [7]. The results of this effort indicate that many applications for SWNTs can be contemplated, *if* higher production rates can be developed while maintaining the integrity of the tube wall. With the Jlab FEL, our preliminary experiments produced high quality SWNTs at 1.5 gm/h. This production rate is limited on the pulse/ chamber design (mainly soot clearing and controlling target temperature) and is not due to FEL limitations. Assuming a linear scale up of production rate with laser power, full-power operation of the FEL would give a soot production rate of 4.5 gm/h. After the current Jlab FEL upgrade is complete, operation at a full power of 10 kilowatts could produce SWNTs at ~ 45 gm/h. It should also be noted that the system has not been optimized for wavelength and several other parameters, suggesting that production rates over 45 gm/h are reasonably possible. For example the FEL output can be tuned to absorption bands of gas phase species (e.g., C_2), which may alter significantly the reaction pathways.

Prior to the present experiments, it was not known whether an FEL or any ultrafast laser system could impact the production of novel materials by PLV. A high power FEL beam has been pursued since 1985[8]. Only recently, has a sustained

kilowatt FEL with "same-cell" energy recovery been available [9]. By sending the electron pulses back through the acceleration system out of phase with the forward beam, 80 % of the energy can be recovered. This allows the FEL at the Thomas Jefferson Accelerator Facility (Jlab) to run at much higher average power than other free electron lasers (i.e., at kilowatts, rather than watts). The present research indicates a bright future for materials synthesis with high power FELs. For more information on the Jlab FEL, readers are directed to (www.jlab.gov) and to ref. 10.

A necessary requirement for the production of SWNTs found by all routes investigated so far appears to be the presence of small metal particles located at an end of an individual tube or bundle of nanotubes. The growth mechanism may well be the Vapor-Liquid-Solid mechanism proposed for filament growth, where the filament is a surface precipitate from a carbon-saturated metal particle [11]. If the particle diameter is small enough ($d < 4$ nm), individual tubes are observed; larger metal particle sizes ($d \sim 10 - 20$ nm) seem to produce bundles of aligned SWNTs that are held together by van der Waals forces. Multiwall carbon nanotubes (i.e., many SWNTs in a nested concentric array) can be produced by CVD with even larger diameter particles [12]. Synthesis routes that utilize the vaporization of carbon, i.e., AD and PLV, incorporate the required metal directly into the carbon feedstock. Metal, or metal carbide particles presumably form by condensation from the metal-carbon vapor. On the other hand, chemical vapor deposition (CVD) methods utilize pre-existing metal particles (supported [5], or unsupported [6]) that may also act as a dehydrogenation catalyst converting hydrocarbon gases into the carbon feedstock at the particle surface. In the present case, Ni-Y and Ni-Co were both added at 1 - 4 at. % to graphite powder and pressed into long 2.5 cm

diameter carbon rods (CarboLex, Inc). Both the Ni-Y and No-Co catalysts produced high yields of tubes of similar quality and diameter distribution. This is interesting, because the prevailing literature suggests that Ni-Y [3] and Ni-Co[4] are, respectively, optimal catalysts for arc discharge (AD) and pulsed laser vaporization (Nd:YAG) growth. In the 3 micron wavelength FEL beam, both catalysts work equally well.

Figure 1 shows a schematic of the experimental setup used at the Jlab FEL in the present experiments. The growth chamber is a fused quartz "T" constructed from a 50 mm diameter tube with a 25 mm diameter side-arm. The 50 mm tube is centered in a 1 meter long, split tube-furnace, and the side-arm protrudes out the side of the furnace near the center of the hot zone. Incident FEL radiation passes through a CaF_2 optical window on the end of the side arm and strikes a catalyzed carbon rod (target) mounted on a rotating and translating quartz rod, as shown in Fig. 1. A jet of pre-heated argon exits through a ~ 0.4 mm diameter hole in a nozzle tip situated 6 mm off the rotating target surface, and about 1 cm upstream from where the laser spot strikes the target. The Ar gas jet deflects the ablation plume almost 90^0 away from the incident FEL beam direction, clearing away the carbon vapor from the region in front of the target. This "side-pumped" geometry was found necessary to harness the high power of the Jlab FEL beam. An overall Ar flow rate of 400 sccm in the 50 mm tube at 500 Torr was maintained by a flow controller (MKS, Inc., model #) and pressure controller (MKS, Inc., model #). The pressure variation was less than ±10 Torr during normal conditions, but could rise to as much as ±50 Torr during high laser power experiments. SWNT soot was collected from a water-cooled copper cold finger at the exhaust end of the 50 mm quartz tube.

For the samples analyzed in this paper, only ~100 W of average laser power was used because of target heating concerns, i.e., less than 1/10th of the available FEL power was incident on the target. If the heat management can be improved, and if the SWNT production rate scales with the incident FEL laser power, then >50 grams/hour might be possible. The target rotation rate was experimentally derived to establish a high "cutting rate" without producing collateral (thermal) damage around the ablation zone. For the initial experimental conditions, we used 1.7 revolutions/sec target rotation.

It is informative to compare some properties of the JLab FEL to a tabletop Nd:YAG laser (Table 1). Our comparison is to the Nd:YAG system at Rice University that first produced bundles of SWNTs at the 100's of mg/day level [4]. This laser's performance is typical of many tabletop Nd:YAG lasers used in PLV systems today. From Table 1, we see that the FEL exhibits a very high repetition rate (75 MHz) train of ultrafast (0.5 ps) low energy (13 μJ) pulses that yield a very high average power beam (~1 kW). The Nd:YAG laser, on the other hand, delivers a low repetition rate (10 Hz) pulse train, where each pulse has a high energy (~1 J) and a relatively long (10 ns) pulse duration. Each laser ablation plume lasts a few msecs and clears the ablation zone before a new pulse arrives [13].

With the FEL beam, a continuous train of75000 laser pulses pump the ablation area during the time of one Nd:YAG pulse. Thus, laser/plume/target interactions are special in the FEL ablation conditions. The high rep rate, short pulses certainly provide a very different energy deposition mechanism than with the Nd:YAG laser. Pulsed Laser Deposition (PLD) research has shown that picosecond-time scale ablation has a fundamentally different mechanism of energy transfer than nanosecond-based ablation.

Picosecond pulses have been found to create a greater energy transfer to the target, reduces energy loss through heat transfer in the target, increases the energy of the ejected species and may hinder particulate formation [14,15]. Note from Table 1, that even though the energy per pulse in the FEL is very small in comparison to the Nd:YAG laser (13 μJ vs 2.5x 10^5 μJ), the peak power in the FEL pulse is comparable to that in the Nd:YAG pulse (10's of megawatts). Also the time-averaged power in the FEL far exceeds the Nd:YAG laser because of the high rep rate (75 MHz) of the FEL compared to 10 Hz for the Nd:YAG laser. With the FEL beam focused on our target, we estimate our resulting peak power density (W/cm^2) was about *1,000 times greater* than for the Nd:YAG case. The FEL average power density (W/cm^2) was about *1,000,000 times greater* than for the Nd:YAG case.

Sample characterization was carried out using SEM, TEM, TPO and Raman scattering, as mentioned above. SEM micrographs were taken using a JEOL JSM 5400 operating at 20KV. Samples were first coated with a thin film of Au to prevent charge accumulation. SEM images (e.g., Fig.2) for the carbon soot produced with NiCo and NiY catalyst show randomly oriented filaments (i.e., bundles) with an average diameter ~10 nm and several micrometers long. The bundle diameters ranged from ~4 - 10 nm for NiY-derived tubes, and from ~4 - 18 nm for NiCo-derived tubes. The metal content in the soot was determined by temperature-programmed oxidation (TPO) to be almost the same as the composition of the target [16]. The metal appears in low-resolution TEM images primarily as carbon-coated metal particles 1 nm – 15 nm in diameter. The TEM image in Fig. 3 is for soot produced with NiY metal (image taken with a JEOL JEM 1200EX microscope at 120 KV). TEM images of the soot produced with NiCo metal

were very similar, and are therefore not shown. High resolution transmission electron microscopy was carried out in a JEOL 2010F (at 100 KV to minimize beam damage) to better reveal the structure of the SWNTs, nanocarbons and metal nanoparticles in the soots. Figure 4 (a, b) show high resolution TEM (HRTEM) images of SWNTs produced by using NiY and NiCo catalyst particles, respectively. The number of tubes within a typical bundle varies from 8 to 200, although we observe many isolated SWNTs in soot produced with both catalysts. From TEM, the individual tube diameter ranged from ~1-1.4 nm. Occasionally, HRTEM images show the presence of peapod structures[17] (Fig. 4b). Fullerenic carbon shells are also observed outside of the SWNTs (Fig 4a). None of the TEM images revealed the presence of double-walled nanotubes (DWNT) or multi-walled nanotubes (MWNT). In the TEM images Fig. 4 (a, b) isolated SWNTs can be seen with perfectly hemispherical fullerenic caps.

Raman scattering spectra of the carbon soots can provide the molecular fingerprint of the SWNT [18-20]. The first Raman spectra of SWNTs were recognized as being due to a resonant scattering process [19]. Later work identified the resonant Raman scattering with absorption between singularities in the electronic density of states due to the one-dimensional character of the SWNT [18]. Since the electronic density of states of the SWNT is diameter-dependent, different laser excitation frequencies excite tubes with different diameters (i.e., only a subset of the tubes can be excited with a single wavelength excitation). The spectra in Fig. 5 (a, b) were taken on soots derived from NiY and NiCo, respectively; four different excitation wavelengths were used (1064 nm, 647.0 nm, 514.5 nm, 488.0 nm) to sample four different subsets of tubes in the sample. The visible Raman spectra were collected at room temperature in the backscattering

configuration using a JY-ISA T64000 spectrometer with an Olympus BH3 confocal microscope (~1 μ diameter focal spot), whereas the IR Raman spectrum using 1064 nm excitation was taken with a BOMEM DA3+ FT-Raman spectrometer. Both spectrometers operated with a spectral slitwidth less than 1 cm^{-1}.

The Raman spectra of SWNTs are well known to exhibit two strong first-order features: the radial displacement band (radial breathing mode), typically found in the region 140-300 cm^{-1}, depending on the SWNT diameter, and a tangential displacement band with maximum intensity near 1590 cm^{-1} that is relatively independent of tube diameter. A somewhat broad, disorder-induced Raman band (or "D-band") in sp^2 carbon is usually observed near 1350 cm^{-1}. This feature is very weak in our spectra; it's strength can either be identified with wall disorder in the SWNTs, to scattering from carbon nanoparticles, or to the presence of a carbon coating on the outside of the tube bundles. The fact that the D-band is weak suggests that the fraction of sp^2 carbon in forms other than SWNTs is low (i.e., multishell carbon particles) and that the wall disorder is also low. The Raman-active radial breathing mode is a clear spectroscopic signature of the cylindrical seamless SWNT, and the diameter-dependence of the mode frequency has been shown to be approximated by ω_R= (224 cm^{-1}. nm)/d(nm) + Δ□, where Δ□~12 cm^{-1} is the correction due to the tube-tube interaction within a bundle [20]. We have used this ω vs. d relation to add a SWNT diameter scale above the respective radial breathing mode regions in Fig. 5 (a, b). It should also be noted that the different shape of the tangential displacement bands (~ 1590 cm^{-1}) in Fig. 5 (a, b) under 514.5 excitation is due to the fact that primarily metallic tubes are being excited at this wavelength in these soots. This observation has been reported previously for PLV and AD materials, and

stems from the nature of the metallic density of states, and the line broadening and shifting due to the electron-phonon interaction [20]. The diameter distributions of the NiY- and NiCo-derived tubes, as revealed by their radial breathing mode frequencies, are remarkably similar, consistent with the results from electron microscopy. Furthermore, the Raman line widths for both the radial and tangential bands in both the NiY- and NiCo-derived samples are comparable, another indication of similar wall integrity in both samples.

Summarizing, electron microscopy and Raman Scattering both indicate that high quality SWNT bundles have been produced by the high power FEL at the Thomas Jefferson National Laboratory. Further work is planned to take advantage of the tunability of the FEL and to pursue even higher production rates commensurate with the full power of the Jlab FEL, which will be upgraded to 10Kwatts in Fall 2002.

Acknowledgments

Work supported by DARPA (DAAD19-00-1-0002), NASA-Langley C&I program, and UPENN NSF MRSEC (#DMR00-79909). We thank Dr. M. Shinn for her assistance and laser expertise and Drs. D. Yates and S.B. Chikkannanavar for their assistance with HRTEM measurements. We also wish to thank the Thomas Jefferson Accelerator Facility for help in setting up the facility and for beam time. We also wish to acknowledge Dr. Fred Dylla of Jlab for his encouragement and support of this project.

References

1. S.Iijima, T.Ichihashi, *Nature* **363**, 603 (1993)

2. D.S. Bethune *et al.*, *Nature* **363**, 605 (1993).

3. C.Journet *et al.*, *Nature* 388, 756 (1997).

4. A. Thess *et al.*, *Science* **273**, 483 (1996).

5. H. Dai, *et al.*, *Chem. Phys. Lett.* **260**, 471 (1996), A. M. Cassell, J. A. Raymakers, J. Kong, H. Dai, J.Phys.Chem.B, **103**, 6484 (1999).

6. P. Nikolaev *et al., Chem. Phys. Lett.* **313**, 91 (1999)

7. K. Tanaka, T. Yamabe, K. Fukui, *The Science and Technology of Carbon Nanotubes*, Elsevier, (Oxford, 1999); M. S. Dresselhaus, G. Dresselhaus, P. C.Eklund, Science of Fullerenes and Carbon Nanotubes; Academic Press: San Diego, 1996

8. R. W. Warren *et al.*, *Nucl. Instrum. Methods Phys. Res. Sect*; **A 237**, 180 (1985).

9. G. R. Neil, *et al.*, *Phys. Rev. Lett.* **84**, 662 (2000).

10. S. V. Benson et al., "Jefferson Lab Free-Electron Laser Starts Operation with Sustained Lasing at the Kilowatt Level," Synchrotron Radiation News, Vol. 13 (4) (July/August 2000).

11. G. G. Tibbet, J. Cryst. Growth, **73**, 431, (1985).

12. M. Endo *et al.*, *Carbon*, **33**, 873, (1995).

13. H. Douglas *et al., App. Phys. A*, **70**, 153 (2000).

14. B. N. Chichkov *et al.*, *App. Phys. A*, **63**, 109 (1996).

15. J. Sturmann *et al., App. Surf. Sci.*, **127**, 59 (1998).

16. The residual catalyst in the SWNT reaction product material was determined by temperature-programmed oxidation (TPO) using a thermogravimetric analyzer (TGA, IGA-3 Hiden UK). In this analysis, all the carbon is assumed converted to

CO/CO_2, and the metal is converted to an oxide. Within the TGA, the carbon SWNT material to be analyzed for metal was maintained in a flow of dry air at 100 sccm, while the temperature was ramped linearly in time (5°C/min) from 25-1000°C.

17. B. W. Smith, M. Monthioux, D. E. Luzzi, *Nature*, **396**, 323 (1998).

18. A. M. Rao *et al.*, Science, **275**, 187 (1997).

19. J. M. Holden, *et al., Chem. Phys. Lett.*, **220**, 186 (1994).

20. M. S. Dresselhaus, P.C. Eklund, *Advances in Physics* **49**, 705 (2000).

Figure Captions:

Figure 1. Schematic of the interaction geometry between the infrared ultrafast pulsed radiation from the FEL (0.5 ps pulses; 75 MHz repition rate, ~ 1 kWatt maximum average power) and the carbon/metal target. The target is a composite rod (e.g., graphite plus a few at% NiY or NiCo) that is rotated and translated while being ablated by the FEL beam. Pre-heated Ar gas is used to clear away the nanotubes from the FEL beam path.

Figure 2. Scanning Electron Microscope (SEM) images of bundles of "as-prepared" SWNTs produced with Ni/Y (1.0 at%/4.0 at%).

Figure 3. Low-resolution Transmission Electron Microscope Images (TEM) images of "as-prepared" SWNT soot produced by the FEL with NiY catalyst.

Figure 4. High Resolution Transmission Electron Microscopy (HRTEM) of "as-prepared" SWNT soot supported on a holy carbon grid, produced with (a) NiY catalysts and (b) NiCo catalysts.

Figure 5. Unpolarized Raman spectra of FEL SWNT soot collected at room temperature: (a) NiY catalysts and (b) NiCo catalysts. The spectra were collected in air under ambient conditions using 1064, 675, 647.1, 514.5, and 488.0 nm radiation.

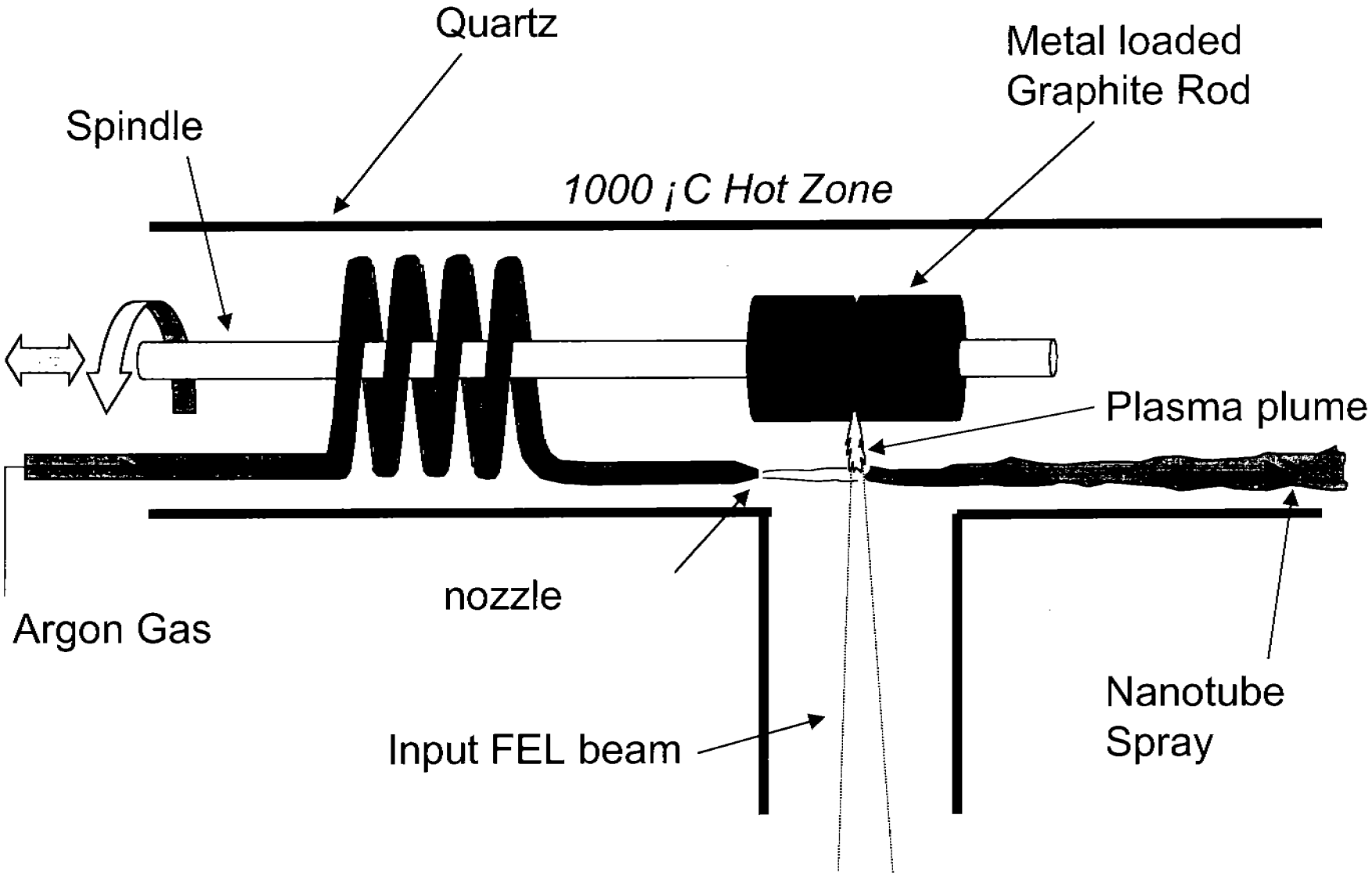
Quartz
Metal loaded
Graphite Rod
Spindle
1000 ¡C Hot Zone
Plasma plume
nozzle
Argon Gas
Input FEL beam
Nanotube
Spray

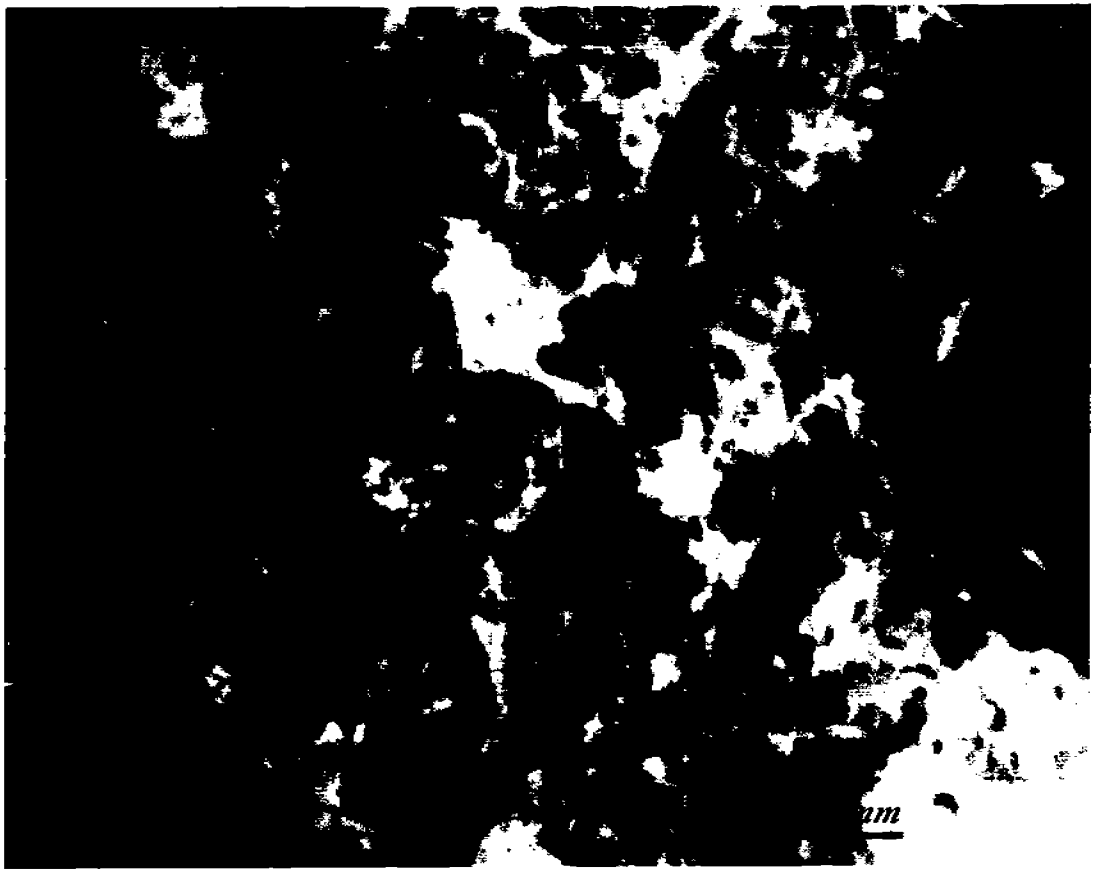

Figure 2

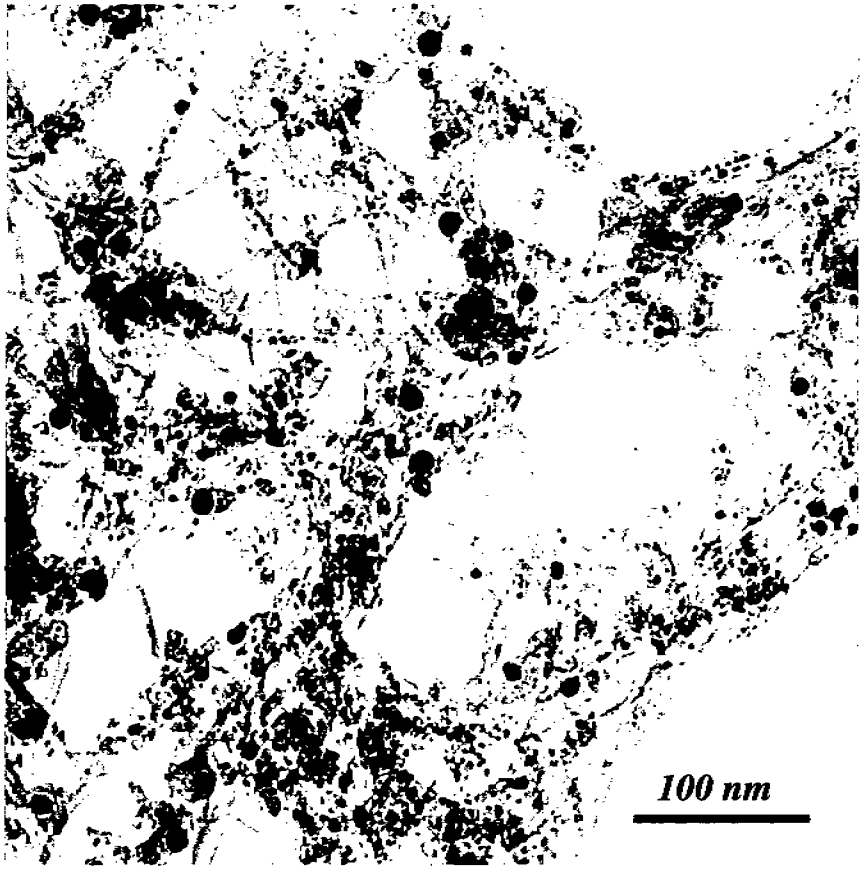

Figure 3

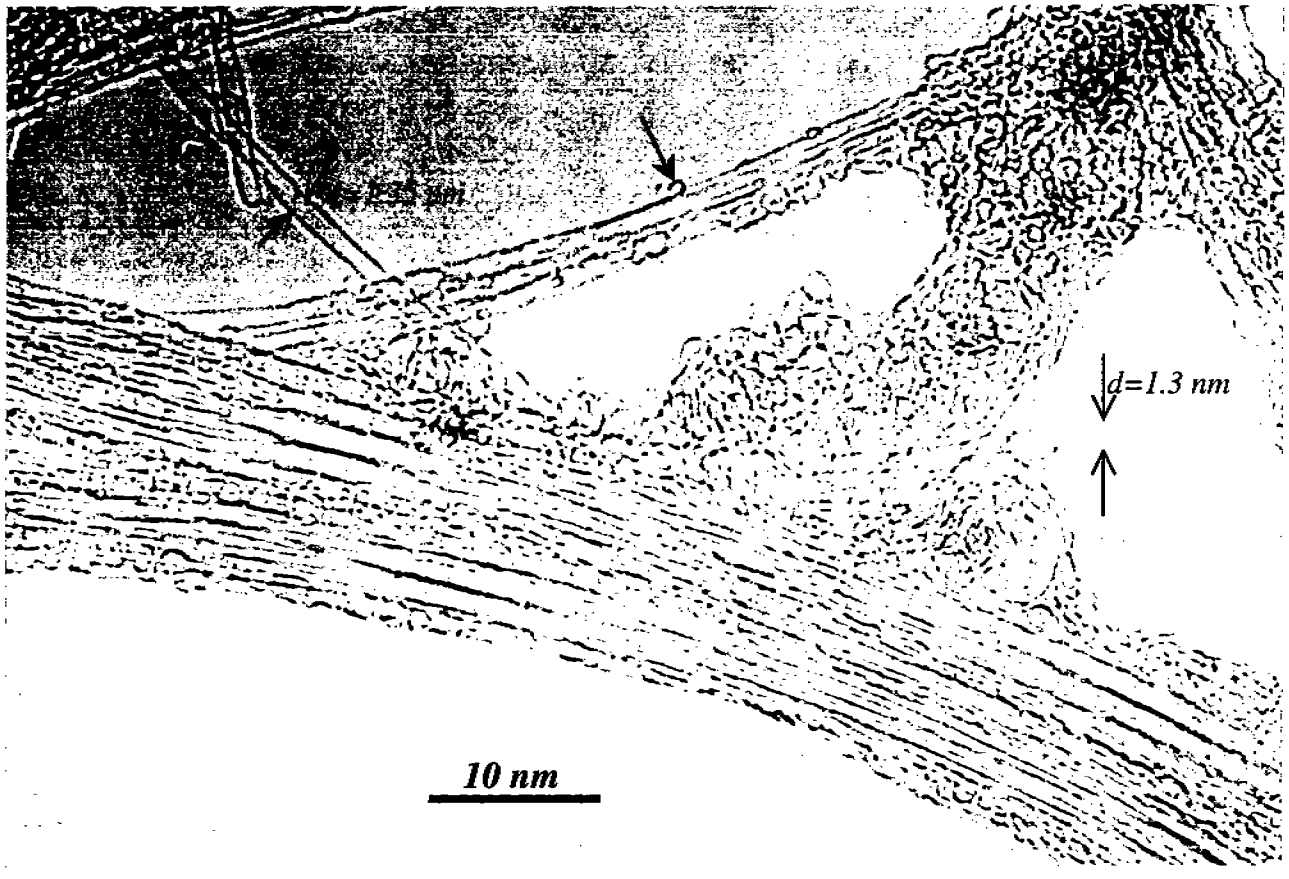

Figure 4 (a)

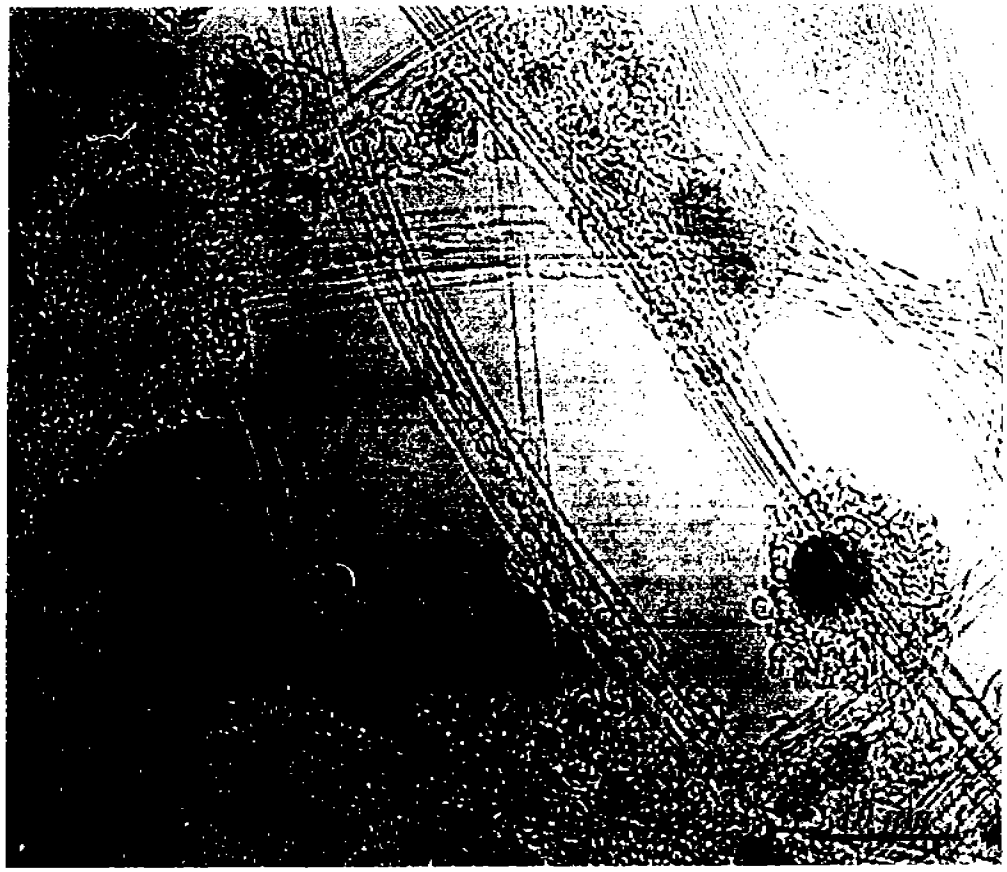

Figure 4 (b)

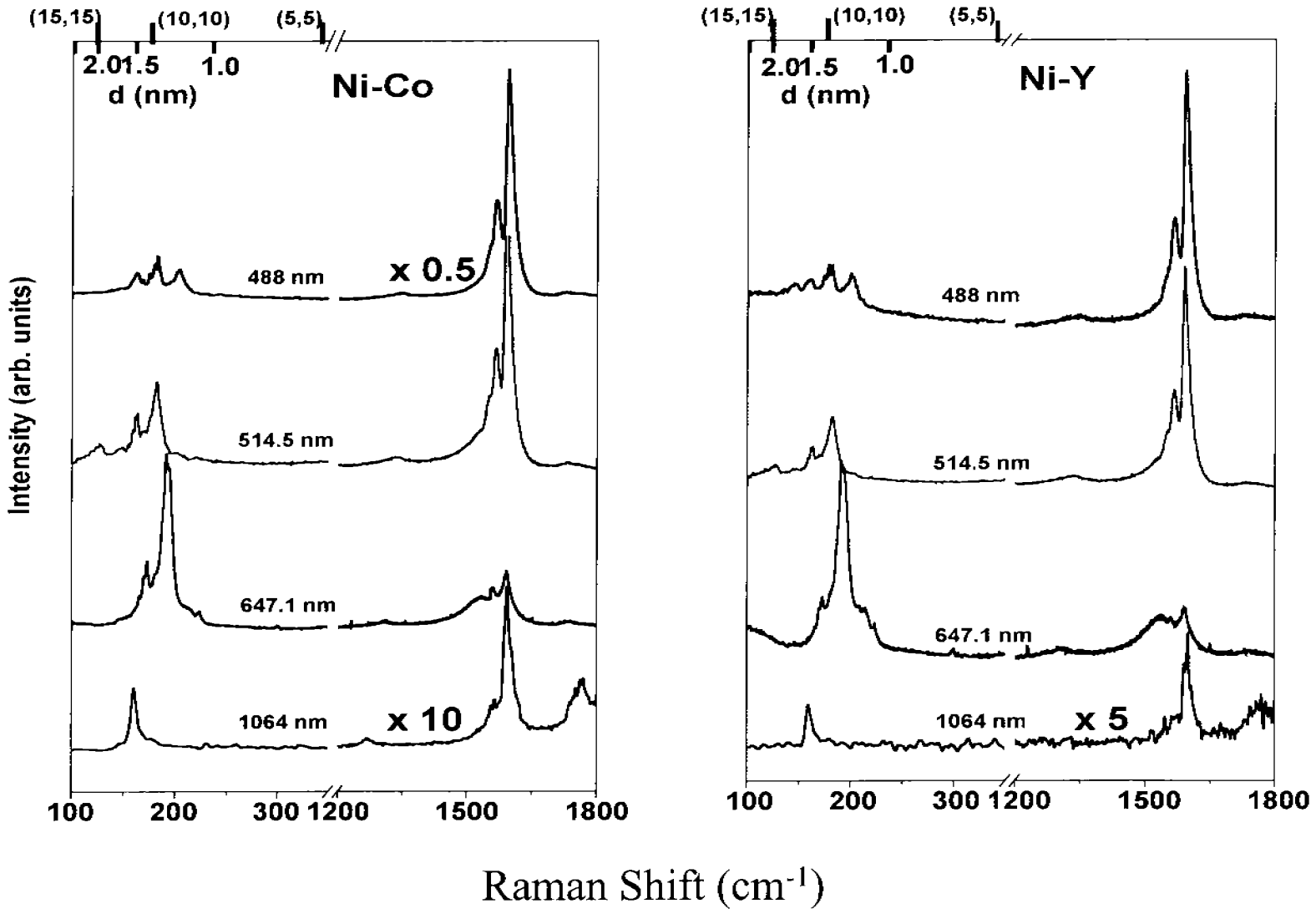

Figure 5 (a) and (b)